Wideband AlN-based SIS devices for frequencies around 700 GHz

C. F. J. Lodewijk, T. Zijlstra, D. N. Loudkov, T. M. Klapwijk, F. P. Mena, and A. M. Baryshev

***Abstract*—We report results on SIS tunnel junctions based on AlN tunnel barriers grown with plasma nitridation from a remote inductively coupled plasma source. Results for the noise temperature are shown and compared to AlO_x results in a ALMA Band 9 mixer. The parameters for AlO_x devices are RnA=25 $\Omega\mu m^2$ with a normal state resistance of 25 Ω and an optimized tuning circuit. For the AlN devices we have RnA = 2.9 $\Omega\mu m^2$ (Jc=71kA/cm^2), A=0.36 μm^2, V_{gap}=2.77 mV, and Rsg/Rn = 14. The data for AlN devices with a not yet optimized tuning circuit show comparable noise temperatures and a flat noise response.**

***Index Terms*—AlN tunnel barriers, heterodyne, nitridation, SIS mixers.**

I. Introduction

THE use of AlN tunnel barriers instead of AlO_x barriers in superconducting tunnel junctions alleviates the problem of tuning out the capacitance and promises to provide an increased band coverage [1]. Although the specifications for Band 9 (602 to 720 GHz) of the atmospheric window at the Atacama Large Millimeter Array (ALMA) can be met with AlO_x, an intrinsically wider band coverage would be beneficial. High critical current-density (low specific resistance) tunnel-junctions are needed to achieve this larger bandwidth. AlO_x barriers have an upper limit [2] of 15 kA/cm^2 (a lower limit of 15 $\Omega\mu m^2$), beyond which excessive sub-gap leakage emerges.

After the initial introduction of AlN [3], various groups have reported successful use of AlN tunnel barriers for mixers at frequencies up to 900 GHz [4], [5]. However, most of the techniques to nitridize aluminium, forming the thin AlN-layer, have shown poor process control and substantial scatter in the achieved current densities [6]. Recently, we have developed a process based on plasma nitridation from a remote inductively coupled plasma source, leading to an excellent degree of control [7].

Manuscript received April 27, 2007. This work was supported by NanoImpuls, the Dutch Research School for Astronomy (NOVA), the Dutch Organisation for Scientific Research (NWO) and the European Southern Observatory (ESO).

C. F. J. Lodewijk, T. Zijlstra, D. N. Loudkov and T. M. Klapwijk are with the Kavli Institute of Nanoscience, Faculty of Applied Sciences, Delft University of Technology, Lorentzweg 1, 2628 CJ Delft, The Netherlands.

F. P. Mena and A. M. Baryshev are with the SRON Netherlands Institute for Space Research and Kapteyn Astronomical Institute, University of Groningen, Landleven 12, 9747 AD Groningen, The Netherlands.

II. AlN Tunnel Barrier Growth

Unlike thermally grown AlO_x, AlN is formed in a nitrogen plasma with a mixture of chemically active species of various energies. It is energetically favorable for Al and O_2 to react into Al_2O_3, whereas it is not favorable for Al and N_2 to form AlN. The latter reaction needs extra energy, which is provided by the plasma.

Most barriers to date have been grown in a parallel plate reactor in which the aluminum is in direct contact with the plasma. Very high current-densities (54 kA/cm^2) have been reached in barriers deposited by reactive sputter deposition [8]. An alternative nitridation-method has been introduced by Kaul *et al.* [9], where a Kaufmann ion source is used to generate a controlled ion flux.

We use an inductively coupled plasma source [10], for which we have chosen to work in the range of high pressures (2×10^{-3} mbar to 1×10^{-1} mbar), in order to have a low energy of the ions. At these higher pressures, the fraction of atomic nitrogen is expected to be large [11], while the energies are as low as a few eV. The substrate is placed on a chuck with a distance with respect to the plasma source, which can be varied from 10 cm to 30 cm. Optionally, the chuck may be DC powered and it can rotate about the height axis.

The AlN barrier is created by first depositing in the usual way a thin (~7 nm) layer of Al on top of Nb in a process chamber. Without breaking the vacuum, the substrate is then transferred to a dedicated nitridation chamber. Subsequently, the Al is exposed to the nitrogen plasma for several minutes, producing a layer of AlN.

III. DC Results and Process Parameters

The devices are fabricated on a quartz substrate. All metal layers are deposited by magnetron sputtering in a Kurt Lesker system. First, a Nb monitor layer is deposited, after which a ground plane pattern is optically defined. Subsequently, a bilayer of Nb/Al is deposited, which is nitridized, followed by a top electrode of Nb. The lateral dimensions of the multilayer of Nb/Al/AlN/Nb are patterned by lift-off. Junctions are defined by e-beam lithography with a negative e-beam resist (SAL-601) layer and etched with a SF_6/O_2 reactive ion etch (RIE) using the AlN as a stopping layer. The junction resist pattern is used as a self-aligned lift off mask for a dielectric layer of SiO_2. A Nb/Au top layer is deposited and Au is etched with a wet etch in a KI/I_2 solution using an optically defined mask. Finally, using an e-beam defined top wire mask pattern,

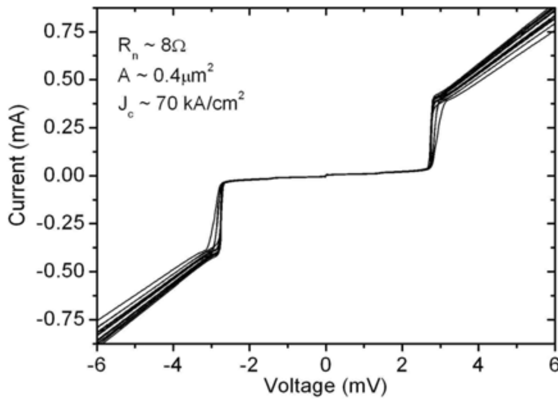

Fig. 1. Current-voltage characteristics of a typical batch of Nb/AlN/Nb junctions. Junction area is about 0.4 μm^2, resulting in a normal resistance, R_n, of 8 Ω (critical current density ~70 kA/cm^2). The Josephson current has been suppressed with a magnetic field. The scatter in R_n is caused by variation in the junction area.

the layer of Nb is etched with a SF_6/O_2 RIE, which finishes the fabrication process.

A set of current-voltage (*IV*) characteristics of a typical batch of SIS devices is shown in Fig. 1. The Josephson current of each junction has been suppressed with a magnetic field. The e-beam defined junction areas A_j are about 0.4 μm^2, while the normal resistance R_n is about 8 Ω. This gives a resistance times area product R_nA of ~ 3 Ωμm^2 (critical current density J_c ~ 70 kA/cm^2). The scatter in the R_n of the devices originates in a variation in A_j. For the observed scatter of ~9% around the mean, the linear uncertainty in the junction definition, which results after reactive ion etching, is about 30 nm.

We have made several batches, varying the nitridation time t_N from 9 to 60 minutes. About half of the batches has been made with a low position of the chuck (30 cm distance to the plasma source) in the nitridation chamber, the other half with a higher position (15 cm distance to the plasma source).

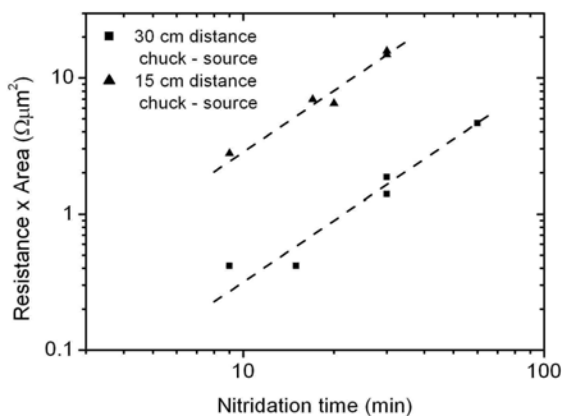

Fig. 2. R_nA product as a function of nitridation time, t_N, for nine different fabricated batches. The squares represent data for a 30 cm chuck-source distance, whereas the triangles indicate a 15 cm chuck-source distance. Dashed lines indicate a dependence $R_nA \propto t_N^{1.5}$, with different prefactors for the two chuck positions.

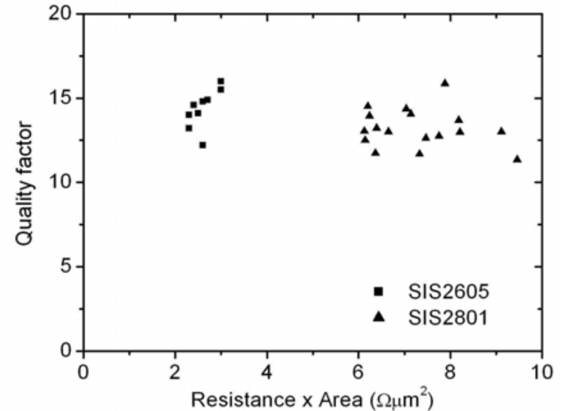

Fig. 3. Quality factor as a function of R_nA product for two batches of Nb/AlN/Nb junctions. The apparent scatter in R_nA within a batch is related to a scatter in junction area.

In Fig. 2, we plot the R_nA product of the batches as a function of t_N for the large chuck-source distance (squares) and for the small chuck-source distance (triangles). The dashed lines indicate a dependence $R_nA \propto t_N^k$, with k = 1.5.

Obviously, there is a systematic dependence on nitridation time, indicating a well-behaving process control. By varying the nitridation time and the chuck position, we can realize any desired R_nA value between 0.5 Ωμm^2 and 10 Ωμm^2.

As shown in Fig. 2, we reach R_nA products as low as ~0.4 Ωμm^2, corresponding to a J_c of 420 kA/cm^2. For such high current densities, heating effects decrease the superconducting gap voltage of the junction in the form of back-bending. Up to about 100 kA/cm^2, this effect is not yet visible.

The quality factor Q, defined as R_{sg}/R_n, where R_{sg} is the subgap resistance, gives an indication of the amount of subgap leakage through the tunnel barrier. For the curves in Fig. 1, Q varies from 10 to 15. The quality factor as a function of R_nA product has been plotted in Fig. 3 for two different batches.

From Fig. 3, it is evident that Q is higher than 10 for all devices down to those with a R_nA of at least 2.5 Ωμm^2 (80 kA/cm^2). The variation in the R_nA within a batch is related to uncertainties in determining A_j: we multiply the measured R_n of a device with the design value of the area. Since there is scatter in the actual value of A_j, reflected in a variation of R_n, the plotted R_nA value shows the same scatter.

IV. RF EVALUATION

All devices incorporate a multisection $Nb/SiO_2/Nb$ microstripline, which tunes out the capacitance of the SIS junction. The transmission efficiency of a device is evaluated using a Fourier Transform Spectrometer (FTS) by measuring the changes in the DC current produced by the incoming light for a chosen bias voltage, selected to be close to the gap voltage.

An AlN-based SIS device is mounted onto a waveguide backpiece designed for Band 9 (600 GHz to 720 GHz) of ALMA. The device has the following parameters: R_n=8.1Ω, A_j=0.36μm^2, Q=14. The microstripline of this device had been

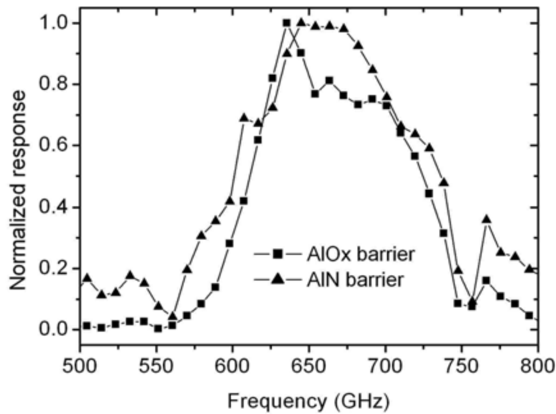

Fig. 4. Normalized photoresponse of two devices, measured with a Fourier Transform Spectrometer (FTS). The triangles are for a device with an AlN tunnel barrier and a non-optimized tuning circuit, whereas the squares show a typical result for an AlO_x based SIS with an optimized tuning circuit. Minima in the response are due to water absorption.

designed for R_n=25Ω and A_j=0.25μm^2. The FTS data for a AlN tunnel barrier, taken at a temperature of 4.2K, are shown in Fig. 4 (triangles). Note that the FTS setup is operated in air. In the same graph, a typical FTS result for an AlO_x based SIS device with an optimized tuning circuit for its parameters R_n=25Ω and A_j=1.0μm^2 is shown.

Obviously, the bandwidth for the AlN based device is larger, despite of the fact that it does not have an optimized tuning circuit. The difference becomes more obvious when the minima due to the water absorption are taken into account, in particular around 560 GHz and 750 GHz.

It is interesting to analyze what one would expect for AlN devices with an optimized tuning circuit. The transmission efficiency, calculated following Ref. 1, for the AlN device of Fig. 4 is shown in Fig. 5 with a full line. The parameters of the actual device have been used. For comparison, the FTS data are shown by triangles. The dashed line shows a calculation of the transmission efficiency for the same SIS junction parameters, but with an optimized tuning circuit. It is evident

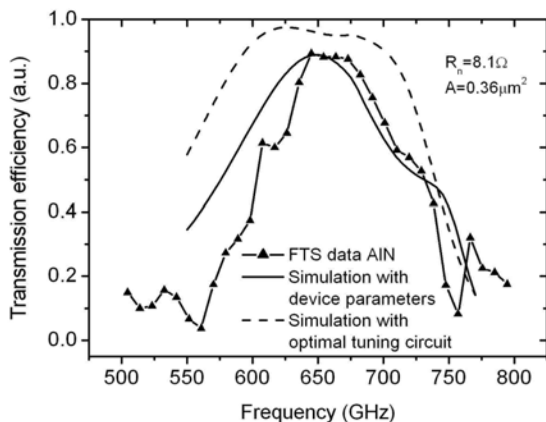

Fig. 5. FTS response of an AlN device (triangles), compared to the simulation (full line), with the non-optimized tuning circuit. The scale for the data is adjusted to match the maximum of the simulation. The dashed line shows the expected response for the same device with an optimized tuning circuit.

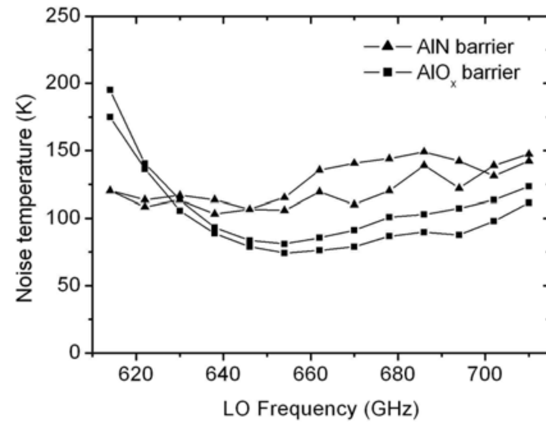

Fig. 6. Uncorrected DSB noise temperature of a SIS mixer with an AlN tunnel barrier (triangles) and the best result obtained for a SIS with an AlO_x tunnel barrier (rectangles), in the frequency range of ALMA Band 9.

that future devices with an optimized circuit will lead to considerable improvement.

The same AlN based device has been mounted in a standard ALMA Band 9 test cartridge. The noise temperature of the mixer, the accompanying optics and the IF chain [12] has been measured using the standard Y-factor method. The resulting uncorrected DSB noise temperatures at different frequencies are presented in Fig. 6 with triangles. In the same graph, the best results obtained with AlO_x based SIS devices are shown with rectangles.

The noise temperature for the AlN device is considerably flatter over the whole range of ALMA Band 9 and compares well with the best results obtained with AlO_x.

V. Conclusion

We have used a new method for AlN tunnel barrier growth, with which we can realize critical current densities of over 100 kA/cm^2. This new method has good process control and reproducibility. Using newly fabricated Nb/AlN/Nb junctions in devices for ALMA Band 9, we have achieved a better bandwidth coverage and a flat noise temperature. By making AlN SIS devices that have an optimized tuning circuit, we expect both bandwidth coverage and noise temperature to improve further.

Acknowledgment

The authors would like to thank O. Noroozian for help with the modeling and B. de Lange and G. Gerlofsma for technical assistance.

References

[1] C.F.J.Lodewijk, O. Noroozian, D.N. Loudkov, T. Zijlstra, A.M. Baryshev, F.P. Mena, and T.M. Klapwijk, "Optimizing superconducting matching circuits for Nb SIS mixers operating around the gap frequency," *IEEE Trans. Applied Superconductivity*, to be published.

[2] R. E. Miller, W. H. Mallison, A. W. Kleinsasser, K. A. Delin, and E. M. Macedo, "Niobium trilayer Josephson tunnel junctions with ultrahigh critical current densities," *Appl. Phys. Lett.*, Vol. 63, 1423 (1993).

[3] T. Shiota, T. Imamura and S. Hasuo, “Nb Josephson junction with an AlN_x barrier made by plasma nitridation,” *Appl. Phys. Lett.*, Vol. 61, 1228 (1992).

[4] J. Kawamura, D. Miller, J. Chen, J. Zmuidzinas, B. Bumble, H. G. LeDuc, and J. A. Stern, “Very high-current-density Nb/AlN/Nb tunnel junctions for low-noise submillimeter mixers,” *Appl. Phys. Lett.*, Vol. 76, 2119 (2000).

[5] J. W. Kooi, J. Kawamura, J. Chen, G. Chattopadhyay, J. R. Pardo, J. Zmuidzinas, T. G. Phillips, B.Bumble, J. Stern, and H. G. LeDuc, “A low noise NbTiN-based 850 GHz SIS receiver for the Caltech submillimeter observatory,” *Int. J. IR and MM waves*, Vol. 21, 1357 (2000).

[6] B. Bumble, H. G. LeDuc, J. A. Stern and K.G. Megerian, “Fabrication of Nb / AI-N, / NbTiN Junctions for SIS Mixer Applications,” *IEEE Trans. Applied Superconductivity*, Vol. 11, 76 (2001).

[7] T. Zijlstra, C. F. J. Lodewijk, ..., D. N. Loudkov, T. M. Klapwijk, “High current-density aluminum-nitride tunnel barriers grown by plasma nitridation from a remote plasma source,” in preparation.

[8] Z. Wang, A. Kawakami, and Y. Uzawa, “NbN/AlN/NbN tunnel junctions with high current density up to 54 kA/cm^2,” *Appl. Phys. Lett.*, Vol. 70, 114 (1997).

[9] A. B. Kaul, A. W. Kleinsasser, B. Bumble, H. G. LeDuc and K. A. Lee, *J. Mater. Res.*, “Aluminum nitride tunnel barrier formation with low-energy nitrogen ion beams,” Vol. 20, 3047 (2005).

[10] M. Weiler, K. Lang, E. Li, J. Robertson, “Deposition of tetrahedral hydrogenated amorphous carbon using a novel electron cyclotron wave resonance reactor,” *Appl. Phys. Lett.*, Vol. 72, 1314 (1998).

[11] T. Czerwiec, F. Greer, and D.B. Graves, “Nitrogen dissociation in a low pressure cylindrical ICP discharge studied by actinometry and mass spectrometry,” *J. Phys. D: Appl. Phys.*, Vol. 38, 4278 (2005).

[12] A. Baryshev, E. Lauria, R. Hesper, T. Zijlstra, and W. Wild, ALMA memo 429.